Dynamics of supercooled liquids: excess wings, β peaks, and rotation–translation coupling

2005 J. Phys.: Condens. Matter 17 1457

(http://iopscience.iop.org/0953-8984/17/10/003)

INSTITUTE OF PHYSICS PUBLISHING JOURNAL OF PHYSICS: CONDENSED MATTER

J. Phys.: Condens. Matter **17** (2005) 1457–1470 doi:10.1088/0953-8984/17/10/003

Dynamics of supercooled liquids: excess wings, β peaks, and rotation–translation coupling

H Z Cummins

Physics Department, City College of the City University of New York, New York, NY 10031, USA

E-mail: cummins@sci.ccny.cuny.edu

Received 27 December 2004, in final form 26 January 2005
Published 25 February 2005
Online at stacks.iop.org/JPhysCM/17/1457

Abstract

Dielectric susceptibility spectra of liquids cooled towards the liquid–glass transition often exhibit secondary structure in the frequency region between the α peak and the susceptibility minimum, in the form of either an 'excess wing' or a secondary peak—the Johari–Goldstein β peak. Recently, Götze and Sperl (2004 *Phys. Rev. Lett.* **92** 105701) showed that a simple schematic mode coupling theory model, which incorporates rotation–translation (RT) coupling, successfully describes the nearly logarithmic decay observed in optical Kerr effect data. This model also exhibits both excess wing and β peak features, qualitatively resembling experimental dielectric data. It also predicts that the excess wing slope decreases with decreasing temperature and gradually evolves into a β peak with increasing RT coupling. We therefore suggest that these features and their observed evolution with temperature may be consequences of RT coupling.

(Some figures in this article are in colour only in the electronic version)

1. Introduction

In liquids at temperatures above the crystal melting temperature T_M, dielectric loss spectra $\varepsilon''(\omega)$ and light scattering susceptibility spectra $\chi''(\omega)$ are dominated by structure in the THz region due to vibrational dynamics. With decreasing temperature, a new feature emerges from the low-frequency side of the vibrational structure and shifts rapidly to lower frequencies. This α relaxation peak is the primary dynamical signature of structural relaxation for which the relevant timescale slows from $\sim 10^{-12}$ s above T_M to $\sim 10^3$ s at the glass transition temperature T_G where the supercooled liquid undergoes structural arrest and enters the non-ergodic glassy state.

Before about 1980 the time or frequency window available to experiments was relatively small and experimental data for the α peak could usually be described satisfactorily by simple empirical functions such as exponential, stretched exponential, and Cole–Davidson functions.

As improvements in experimental techniques extended the accessible time or frequency region, deviations from these simple fitting functions became increasingly apparent, revealing that α decay is the final stage of complex structural relaxation dynamics. Additional features have been repeatedly observed in dielectric susceptibility spectra on the high-frequency wing of the α peak, and are called secondary structure. One type is generally referred to as the 'excess wing'; another is the secondary peak—the JG (Johari–Goldstein) β peak. Various characteristics of these features and their evolution with decreasing temperature have been reported, and several empirical fitting approaches have been described. Several possible mechanisms have been suggested to explain their occurrence including internal molecular motions and cooperative dynamics, but no underlying physical mechanism has yet been definitely identified that is capable of explaining the occurrence of these features and their evolution with temperature.

While we will focus on the appearance of secondary structure in dielectric spectra, similar features have also been observed in other types of experiment including light scattering [1] and mechanical loss measurements [2]. Recently, Brodin *et al* studied the α relaxation spectra of several glass-forming materials using both dielectric and photon correlation spectroscopies, and found that the magnitude of the secondary relaxation processes relative to the primary α peak is much smaller in the light scattering spectra than in the dielectric spectra [1].

The dielectric susceptibility of liquids of anisotropic molecules is dominated by orientational dynamics, so the contribution of density fluctuations is routinely ignored. The α peak is assumed to represent the decay of orientational correlations, and the excess wing is attributed to unspecified 'secondary relaxation processes'. But density dynamics can also modify the orientational dynamics as a consequence of the coupling of rotation and translation, the RT coupling effect that also underlies phenomena such as flow birefringence.

Rotation–translation (RT) coupling has long been known to play a role in the form of light scattering spectra of liquids of strongly anisotropic molecules. The 90° depolarized light scattering spectrum $I_{\mathrm{VH}}(\omega)$ of strongly anisotropic liquids exhibits a narrow dip centred at $\omega = 0$ (the Rytov dip) due to RT coupling [3], and the 90° polarized spectrum $I_{\mathrm{VV}}(\omega)$ of salol has recently been shown to exhibit a weak low-frequency feature that is also attributable to RT coupling [4]. These effects arise from modification of the orientational dynamics via interaction with translational motion of the molecules. (For detailed discussions of the effects of RT coupling on light scattering spectra, see the series of papers by Pick and co-workers [5].) It is therefore worthwhile to consider the possibility that the excess wing and β peak phenomena might also be attributable to RT coupling.

Recently, Götze and Sperl [6] showed that a simple schematic mode coupling theory (MCT) model that incorporates RT coupling successfully describes the nearly logarithmic decay observed in optical Kerr effect data [7]. This model was also found to exhibit α peaks having excess wing or β peak features, qualitatively resembling experimental dielectric data, suggesting that both of these features may be consequences of rotation–translation coupling [6].

In this paper we will compare the secondary relaxation structure observed in experimental dielectric data for the glass-forming material propylene carbonate with predictions of a schematic MCT model that includes RT coupling. The comparison is qualitative, intended to demonstrate that secondary relaxation may be a consequence of RT coupling. No actual MCT analysis of the data is currently possible, since the secondary structure observed experimentally occurs at temperatures too low for accurate MCT analysis to be performed.

2. Experimental overview

Structural relaxation dynamics extends over a time or frequency region that can span more than ten decades. Until fairly recently, no experimental technique could span a range large enough

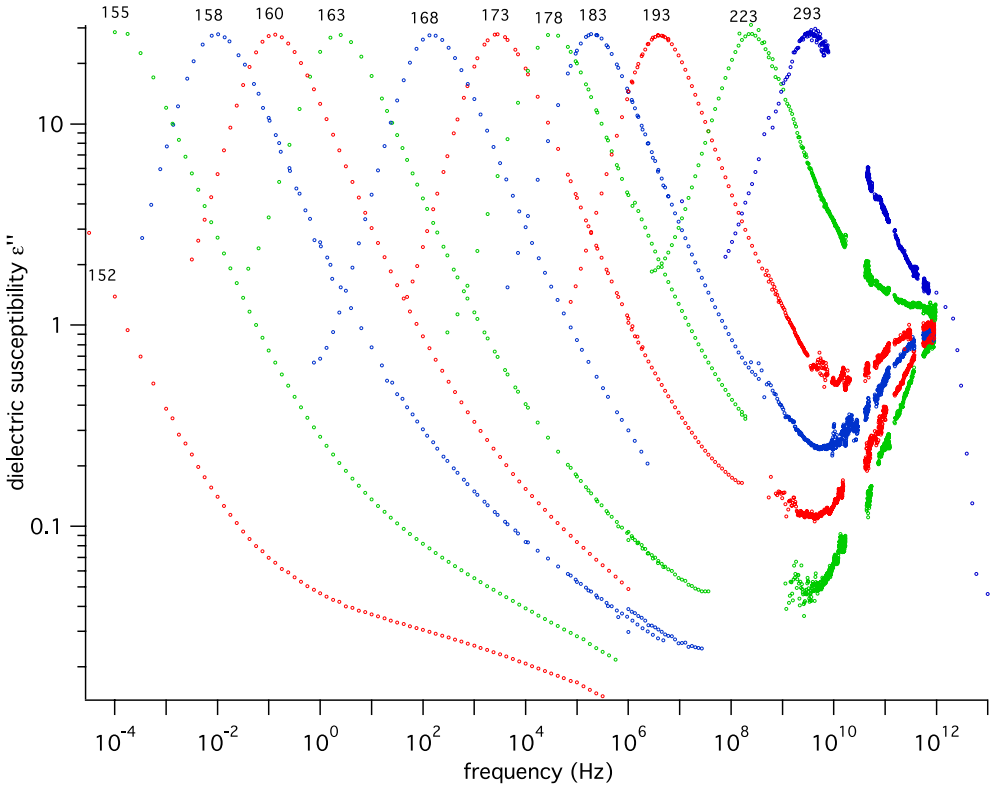

Figure 1. Dielectric loss spectra $\varepsilon''(\omega)$ of propylene carbonate in the temperature range 293–152 K. (Data provided by Lunkenheimer.) For the lowest three temperatures there is a clearly visible excess wing on the high-frequency side of the α peak which is evolving into an incipient β peak at 152 K. The high-frequency region of the vibrational peak is shown for the 293 K spectrum which was extended up to 10^{13} Hz with far-infrared measurements.

for exhibiting all the features of interest. However, Lunkenheimer, Loidl, and co-workers have extended the frequency range of dielectric spectroscopy by combining conventional dielectric techniques with submillimetre-wave spectroscopy, enabling them to map out the dielectric loss spectrum over more than 18 decades in frequency, from below the α peak through the minimum and up through the high-frequency vibrational peak [8]. In figure 1 we show dielectric loss spectra $\varepsilon''(\omega)$ for PC (propylene carbonate) provided by Lunkenheimer. This figure illustrates the various regions of interest in the $\varepsilon''(\omega)$ spectrum as well as their evolution with temperature. While most of the spectra shown end at 10^{12} Hz, the 293 K spectrum has been extended up to 10^{13} Hz with far-infrared measurements, revealing the high-frequency side of the vibrational peak.

The existence at low temperatures of a secondary β relaxation peak at frequencies above the primary α peak was recognized and studied extensively in the 1960s. As early as 1951, Davidson and Cole noticed that the dielectric loss spectra of glycerol, propylene glycol, and n-propane all exhibited a second dispersion at frequencies above $1/\tau_\alpha$ even though their available frequency range was limited to the range 20 Hz–5 MHz [9]. β peaks were also found to occur below T_G in many polymers with mobile side-chains and were initially attributed to motion of the side-chains in the otherwise rigid polymer matrix. When they were subsequently also

found to occur in polymers without side-chains, the motions were attributed to 'crankshaft motion' of parts of the main polymer chains [10].

In 1969, Goldstein proposed the potential energy barrier description of supercooled liquids and suggested that cooperative motion of molecules in the nearly rigid matrix can give rise to a distribution of relaxation times that could lead to secondary relaxation peaks [11]. In subsequent dielectric studies, Johari and Goldstein observed β peaks in a number of liquids composed of rigid molecules [12–14]. They concluded that 'β relaxation is a characteristic relaxation of liquids in or near the glassy state, and has its origin in the same intermolecular forces that are responsible for the glass transition itself' [14].

Investigation of the excess wing phenomenon began later. In 1974, Wong and Angell plotted conductivity data $\sigma(\omega) = \omega\varepsilon''(\omega)$ versus ω for glycerol on a log–log scale. They found that at high frequencies $\sigma(\omega)$ increases approximately linearly with ω, suggesting that far above the alpha peak $\varepsilon''(\omega)$ approaches a frequency-independent constant value, usually called the 'constant loss' [15]. Similar plots of conductivity data for several materials were published recently by Lunkenheimer and Loidl [16]. Sokolov *et al* have observed an extensive range of constant loss in the light scattering susceptibility spectrum of the polymer PIB [17]. The appearance of a constant loss region in susceptibility spectra is equivalent to the appearance of a region of nearly logarithmic decay in the corresponding correlation function.

Leheny and Nagel analysed the α peak and excess wing in the dielectric susceptibility data for several liquids and found that in the region above the peak $\varepsilon''(\omega)$ could be fitted by the sum of two power laws: $\varepsilon''(\omega) = C_1\omega^{-\beta} + C_2\omega^{-\sigma}$ with $\sigma < \beta$, and that the excess wing slope σ decreases as T decreases [18]. Extrapolating their fits to low temperatures, they suggested that there exists a temperature $T_0 < T_G$ at which $\sigma \to 0$ and $\omega_{peak} \to 0$ simultaneously, which they interpreted as indicating a possible thermodynamic transition. This interpretation remains controversial, but their experimental observation of a temperature-dependent excess wing slope is independent of the particular interpretation.

Rössler and co-workers have reported several detailed studies of the susceptibility spectrum in materials having an excess wing but no β peak (which they designated as type A—e.g. glycerol), and in materials having a β peak (designated as type B—e.g. toluene) [19–21]. However, it is not clear that this distinction is generally applicable.

Lunkenheimer and co-workers have reported broadband dielectric spectra of glycerol [22–26], PC [25, 27, 28], and ethanol [29]. These experiments revealed both excess wing and β peak features as discussed further in the next section. Furthermore, in [30], ageing experiments on PC and glycerol at temperatures below T_G revealed an excess wing that gradually transforms with time into a β peak. Blochowicz and Rössler have found that the dielectric spectra of a binary molecular glass former exhibits an excess wing that gradually transforms into a β peak when the concentrations of the components are changed [31]. Recently, Oh and Hwang have observed that the high-frequency wing of the dielectric spectrum of glucose–water mixtures at equilibrium transforms into a distinct β peak either with decreasing temperature or with decreasing water content [32]. In [26], Ngai *et al* suggested that the excess wing might generally be a manifestation of the β peak phenomenon rather than a distinct dynamical process. The relation between the excess wing and the β peak has also been discussed recently by Ngai and Paluch [33].

The distinction between type A and type B glass formers has also been called into question by two experiments in which dielectric susceptibility measurements were performed with applied hydrostatic pressure [34, 35]. In these experiments, $\varepsilon''(\omega)$ exhibited an excess wing but no β peak at low pressures, while at pressures above ~400 MPa a distinct β peak appeared and became increasingly prominent with increasing pressure. This result again suggests that the β peak and the excess wing may be manifestations of the same dynamical process, appearing

as a separate β peak when some physical parameter becomes sufficiently strong. In this paper, we suggest that the relevant parameter may be the rotation–translation (RT) coupling constant which becomes stronger as pressure increases or temperature decreases, both of which produce increases in the density. It is also expected to be larger for liquids composed of more elongated molecules.

3. Empirical analyses

3.1. The α relaxation process

If the dynamical variable being probed in an experiment is represented by $X(t)$ (e.g. a Fourier component of the density fluctuation $\rho_q(t)$ or a component of the local molecular orientation $Q(t)$), then the time dependence of $X(t)$ can be conveniently described by its normalized autocorrelation function $\phi_X(t) = \langle X^*(t)X(0)\rangle/\langle|X(0)|^2\rangle$. The simplest empirical model for $\phi(t)$ is the Maxwell–Debye exponential relaxation function $\phi(t) = \exp(-t/\tau_\alpha)$ for which the spectrum $S(\omega)$, the real part of the Fourier transform of $\phi(t)$, is a Lorentzian centred at $\omega = 0$, and the susceptibility spectrum $\chi''(\omega)$ or $\varepsilon''(\omega)$, which is related to $S(\omega)$ by the classical fluctuation-dissipation theorem $\chi''(\omega) = (\omega/2kT)S(\omega)$, is also a Lorentzian: $\chi''(\omega) = \chi_0\omega\tau/(1+\omega^2\tau_\alpha^2)$, which has a peak (the α peak) at $\omega_{\text{peak}} = \tau_\alpha^{-1}$. In practice, $\phi(t)$ is usually not well described by the Maxwell–Debye exponential model, but can frequently be fitted by the KWW (Kohlrausch–Williams–Watts) stretched exponential function

$$\phi(t) = \exp(-[t/\tau_\alpha]^\beta) \tag{3.1}$$

where $\beta \leqslant 1$ is the KWW stretching coefficient.

There is no analytic Fourier transform of (3.1), so the spectrum $S(\omega)$ and susceptibility spectrum $\chi''(\omega)$ are represented either by the numerical Fourier transform of (3.1) or by a related empirical function such as the approximately equivalent Cole–Davidson (CD) function for which the susceptibility spectrum is

$$\chi''_{\text{CD}}(\omega) = \chi_0 \,\text{Im}[1 - (1 + \text{i}\omega\tau)^{-\beta_{\text{CD}}}]. \tag{3.2}$$

Both the KWW and CD functions have been widely used to analyse dielectric, light scattering, and neutron scattering data. Lunkenheimer and co-workers analysed α peaks using both Fourier-transformed KWW functions and CD functions for glycerol [22, 24] and for PC [25–28]. For PC, they noted that for all temperatures investigated, the KWW fit is of lower quality than the CD fit [27].

3.2. The excess wing

For PC, at temperatures below ∼173 K, as seen in figure 1, the high-frequency wing of the α peak exhibits a decrease in slope where the CD or KWW fit begins to fall below the experimental data, indicating the presence of an excess wing. In figure 2 we show the PC $\varepsilon''(\omega)$ spectrum of figure 1 for $T = 160$ K with a fit to the sum of a CD function (equation (3.2)) plus a power law: $\varepsilon''(\omega) = \varepsilon''(\omega)_{\text{CD}} + B\omega^a$ for which $a \sim 0.21$. (The power law has been multiplied by a low-frequency exponential cutoff $\exp[-1/\omega\tau]$ to avoid having it dominate the low-frequency α peak region.) Similarly, for glycerol below ∼234 K, an excess wing becomes visible. Lunkenheimer *et al* were able to fit the glycerol spectra by combining a KWW fit for the α peak region with a power law fit to the high-frequency wing [36]. Similarly, in analysing light scattering spectra of toluene, Wiedersich *et al* fit their $\chi''(\omega)$ spectra with the sum of a CD function and a power law [37].

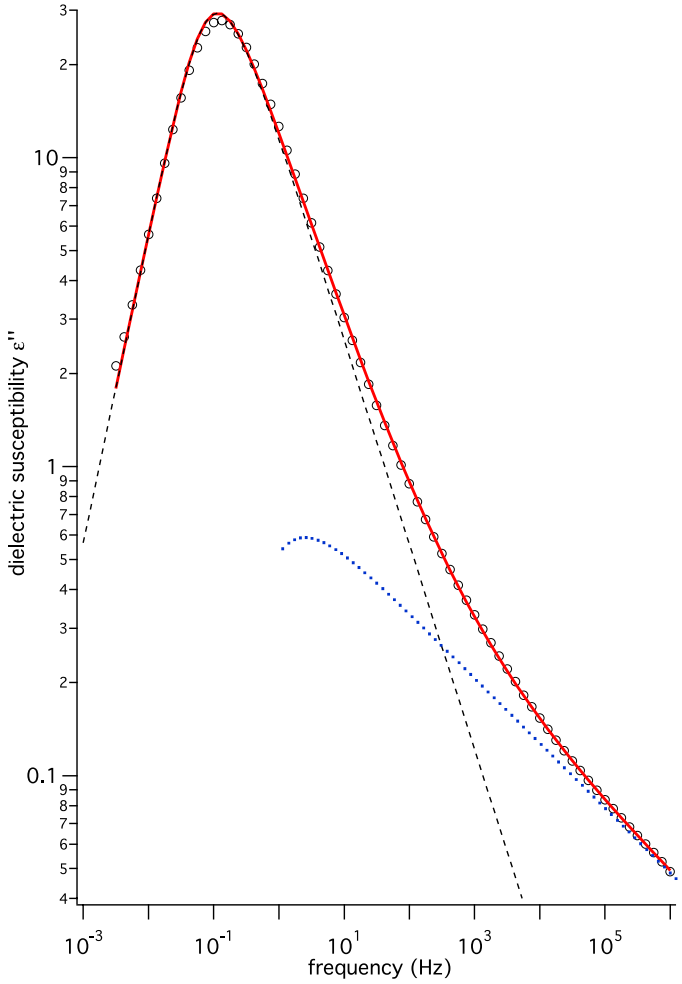

Figure 2. The dielectric loss spectrum $\varepsilon''(\omega)$ of PC at $T = 160$ K with a phenomenological fit to the sum of a Cole–Davidson function (– – –) plus a power law excess wing (· · · · · ·). The power law contribution has been multiplied by a low-frequency exponential cutoff $\exp[-1/\omega\tau]$ to prevent distorting the α peak. Parameters found in the fit to $\varepsilon''(\omega) = I_{\rm CD}\,{\rm Im}[1-(1+{\rm i}\omega\tau)^{-\beta}] + I_{\rm pow}\omega^{-a}{\rm e}^{-(1/\omega\tau)}$ were: $I_{\rm CD} = 71.4$; $\tau(s) = 1.909$; $\beta = 0.663$; $I_{\rm pow} = 0.881$; $a = 0.21$.

3.3. The JG β peak

The β peak can often be fit with a phenomenological fitting function such as the Cole–Cole function

$$\chi''_{\rm CC}(\omega) = \chi_0\,{\rm Im}[1-({\rm i}\omega\tau_\beta)^a]^{-1} \tag{3.3}$$

that can be combined with other functions to describe the full spectrum. In figure 3 we show the PC $\varepsilon''(\omega)$ spectrum for $T = 153$ K fitted with the sum of CD and CC functions.

In a recent series of papers, Lunkenheimer *et al* have re-examined the high-frequency wing of dielectric loss spectra of PC, glycerol, ethanol, propylene glycol, and salol [26, 28–30]. They have shown that, for all cases, the spectrum can be fitted by combining a CD or Fourier-transformed KWW function for the α peak with a Cole–Cole function, even if no distinct β peak is visible in the spectrum. They note that: 'Until recently, it was commonly

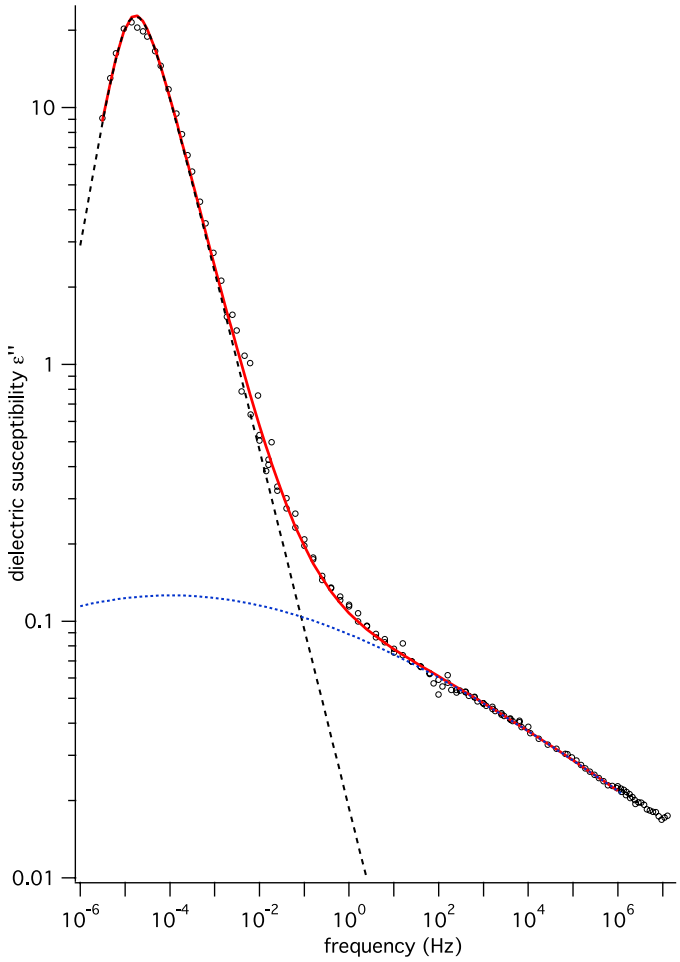

Figure 3. The dielectric loss spectrum $\varepsilon''(\omega)$ of PC at $T = 153$ K with the phenomenological fit to the sum of Cole–Davidson (- - - -) and Cole–Cole ($\cdots\cdots$) functions. The parameters found in the fit to $\varepsilon''(\omega) = I_{\rm CD}\,{\rm Im}[1-(1+{\rm i}\omega\tau)^{-\beta}] + I_{\rm CC}\,{\rm Im}[1-({\rm i}\omega\tau_\beta)^a]^{-1}$ were: $I_{\rm CD} = 53.84$; $\tau_{\rm CD} = 1.24\times10^4$ (s); $\beta_{\rm CD} = 0.697$; $I_{\rm CC} = 2.413$; $\tau_\beta = 9.259\times10^3$ (s); $a = 0.1323$.

assumed that the excess wing and β relaxation are due to different microscopic processes. Indeed, strong indications were obtained that the excess wing is simply the high-frequency flank of a β peak, submerged under the dominating α peak' [26]. Similarly, Brand *et al* [29] were able to fit the excess wing in ethanol, where no β peak is observed, by adding a weak β peak to the strong α peak, with the sum of the two exhibiting an α peak and excess wing only. Comparing figures 2 and 3, the distinction between materials exhibiting an excess wing or a β peak is clearly questionable since these two fits represent the same material at temperatures differing by only 7 K. A similar evolution of the excess wing into an incipient β peak can be seen in the dielectric spectrum of salol between 222 and 204 K, shown in figure 4 of Kudlik *et al* [38].

3.4. Rössler's analysis

Rössler and co-workers have reported several detailed studies of susceptibility spectra in materials having either an excess wing or a β peak [1, 19–21]. They have introduced a new

empirical fitting function, a generalized gamma distribution, which represents a continuous distribution of relaxation times. Their distribution function, $G(\ln \tau)$, is able to fit the complete susceptibility spectrum for several different materials with the variation of four parameters: two to fit the α peak, and two others to describe the onset and slope of the excess wing. Their fits to the glycerol data of Lunkenheimer *et al* are shown in [21].

4. Mode coupling theory

The mode coupling theory (MCT) was proposed in 1984 by Bengtzelius *et al* [39] as a model for the dynamics of liquids approaching the liquid–glass transition. MCT is a microscopic theory that starts from Hamilton's equations of motion for the molecular coordinates and momenta and uses the Zwanzig–Mori projection operator formalism to derive equations of motion for the macroscopic variables. In its basic version, MCT includes only the density fluctuation modes $\rho_q(t)$ with autocorrelation functions $\phi_q(t)$ (the dynamic structure factors) and their nonlinear interactions with other density fluctuation modes. Starting from the classical microscopic Hamiltonian equations of motion for the molecular centre-of-mass positions and momenta and employing the Zwanzig–Mori projection operator formalism, MCT gives exact equations of motion for the correlators $\phi_q(t)$:

$$\frac{\partial^2}{\partial t^2}\phi_q(t) + \gamma_q \frac{\partial}{\partial t}\phi_q(t) + \Omega_q^2 \phi_q(t) + \Omega_q^2 \int_0^t m_q(t-t')\frac{\partial}{\partial t'}\phi_q(t')\,\mathrm{d}t' = 0. \quad (4.1)$$

The major programme of MCT computes the memory functions $m_q(t)$ in these equations, which involves making several simplifying approximations [40, 41]. In these calculations, the memory function $m_q(t)$ is expressed in terms of sums of products of pairs of correlators with the form $V(q, q', q'')\phi_{q'}(t)\phi_{q''}(t)$ where the coupling coefficients $V(q, q', q'')$ are determined by the intermolecular potential. Solution of the resulting set of coupled equations leads to the prediction of structural arrest at the MCT crossover temperature T_C and two-step relaxation with asymptotic power law regions [40]. For most molecular liquids, however, the intermolecular potentials are too complicated to allow the nonlinear coupling constants to be calculated reliably. Therefore, comparisons of experimental data with MCT predictions are frequently carried out using either the generic asymptotic power law predictions of MCT that follow from asymptotic expansions close to T_C [42] or else with simplified schematic versions of equation (4.1) using only one or two correlators. The simplest useful schematic model is the one-correlator F_{12} model [43], i.e. equation (4.1) with the subscript (q) suppressed, with the memory function $m(t)$ given by

$$m(t) = V_1\phi(t) + V_2\phi^2(t) \quad (4.2)$$

where the two coupling constants V_1 and V_2 are treated as fitting parameters.

While many sets of experimental data on the liquid–glass transition of various materials have been analysed by fitting to the basic MCT predictions [42], a problem arises in principle for liquids composed of strongly anisotropic molecules because the basic MCT is a theory of density fluctuations while, in such liquids, orientational dynamics often dominates the measured data. This problem has usually been sidestepped with the assertion that since orientation and translation are strongly coupled, the forms of $\phi(t)$ for the density and orientation correlators should be similar. While this assertion should be valid very close to T_C, it is not generally correct. Formal extensions of MCT to include both translational and orientational dynamics have been described in several recent publications [44] but these formulations, in their present form, are not easily used to analyse experimental data.

4.1. The Sjögren model

A related problem occurs in the analysis of incoherent neutron or light scattering experiments where the variable being probed is single-particle dynamics represented by the self-correlation functions $\phi_q^s(t)$. Since single-particle motion interacts with density fluctuations, the memory function in the equation of motion for $\phi_q^s(t)$ involves products of $\phi_q^s(t)$ with density correlators $\phi_q(t)$ [45]. Van Megen *et al* have employed incoherent light scattering techniques to determine the self-intermediate-scattering function of hard sphere colloidal suspensions [46], and Sperl has recently shown how the MCT analysis including the interaction of $\phi_q^s(t)$ and $\phi_q(t)$ can successfully explain the data including a region of nearly logarithmic decay [47].

Since this theory is too difficult to apply to molecular liquids (as opposed to hard sphere colloids), Sjögren proposed a simplified schematic model in 1986 in which the density fluctuation dynamics is represented by the F2 model, i.e. equation (4.1) with $m(t) = V_2\phi^2(t)$, with a second auxiliary correlator $\phi_A(t)$ representing the single-particle dynamics [48]. Götze and Sperl [6] used an extended version of the Sjögren model in which the density fluctuation dynamics is represented by the F12 model of equation (4.2) in their analysis of experimental OKE data for liquids composed of anisotropic molecules. In this application of the Sjögren model, the auxiliary correlator $\phi_A(t)$, which is coupled to $\phi(t)$, represents the orientational dynamics. The coupled equations of motion and memory functions for the density correlator $\phi(t)$ and the auxiliary (orientational) correlator $\phi_A(t)$ are given by

$$\frac{\partial^2}{\partial t^2}\phi(t) + \gamma\frac{\partial}{\partial t}\phi(t) + \Omega^2\phi(t) + \Omega^2\int_0^t m(t-t')\frac{\partial}{\partial t'}\phi(t')\,\mathrm{d}t' = 0 \tag{4.3a}$$

$$m(t) = V_1\phi(t) + V_2\phi^2(t) \tag{4.3b}$$

$$\frac{\partial^2}{\partial t^2}\phi_A(t) + \gamma_A\frac{\partial}{\partial t}\phi_A(t) + \Omega_A^2\phi_A(t) + \Omega_A^2\int_0^t m_A(t-t')\frac{\partial}{\partial t'}\phi_A(t')\,\mathrm{d}t' = 0 \tag{4.3c}$$

$$m_A(t) = V_A\phi_A(t)\phi(t). \tag{4.3d}$$

Equations (4.3*a*) and (4.3*b*) for $\phi(t)$ result in a line of conventional MCT glass transition singularities in the (V_1, V_2) plane given by

$$V_1^c = (2\lambda - 1)/\lambda^2; \qquad V_2^c = 1/\lambda^2 \tag{4.4}$$

where λ is the MCT exponent parameter ($0.5 \leqslant \lambda \leqslant 1$). ($\lambda$, in turn, determines the MCT critical exponents a and b.) With decreasing T, the point (V_1, V_2) moves towards this line; T_C corresponds to the value of T at which the (V_1, V_2) point intersects the transition line (structural arrest). The intersection then determines the value of the MCT exponent parameter λ through equation (4.4). If V_A is sufficiently large, the orientational correlator $\phi_A(t)$ will also undergo a glass transition at T_C because of the nonlinear coupling term $V_A\phi_A(t)\phi(t)$ in equation (4.3*d*). If V_A is too small, then the orientational dynamics would not arrest; the solid phase at $T < T_C$ would be a disordered plastic crystal, i.e. a glass with translational motion frozen but not orientational motion. The density fluctuation dynamics, however, is unaffected by the value of V_A.

The Sjögren model includes seven free parameters; Ω, Ω_A, γ, γ_A, V_1, V_2, and V_A. Four of these, Ω, Ω_A, γ, and γ_A, primarily determine the short-time microscopic transient dynamics of ϕ and ϕ_A and set the timescale. In carrying out fits to data sets, one should require that the state point (V_1, V_2) moves along a smooth trajectory as T changes, and that all seven fitting parameters have smooth temperature dependences.

Götze and Sperl [6] showed that equations (4.3) provide excellent fits to the OKE (optical Kerr effect) data of Fayer, Hinze *et al* [7, 49] for BZP and salol which exhibited a surprising region of nearly logarithmic decay. Logarithmic decay is not expected within the basic MCT,

i.e. the idealized theory for density fluctuations only (except for special points in the parameter space in the vicinity of cusp bifurcations), either as the set of equations (4.1) with each m_q given by the sum of products of correlators, or else a schematic version such as the F_{12} model. The Sjögren model introduces another degree of freedom beyond the density fluctuations which can represent either orientational dynamics or single-particle dynamics, and it is the spectrum of that new variable, which is coupled bilinearly to the density fluctuations, that exhibits the nearly logarithmic decay. Thus, the intermediate nearly logarithmic decay region found by Fayer and Hinze was shown to occur in the orientational correlator $\phi_A(t)$ as a consequence of RT coupling. The Sjögren model was also used by Wiebel and Wuttke to analyse depolarized light scattering in benzene [50], and by Ricci *et al* to analyse OKE data for benzene [51]. Although benzene does not exhibit a glass transition, both groups were nevertheless able to find good fits to their data in a limited temperature range and found that the three coupling constants V_1, V_2, and V_A all increase monotonically with decreasing temperature.

The Sjögren model is somewhat unphysical in that the orientational dynamics is modified by coupling to translational dynamics, but the translational dynamics is independent of the orientational dynamics. Physically, one would expect RT coupling to modify both translational and orientational dynamics. However, this lack of symmetry is unimportant for our purposes since we use only the orientational correlator to describe OKE, dielectric, and depolarized light scattering data. There is also an advantage to the lack of symmetry since one can solve the equations for a given set of parameters and then compare $\phi_A(t)$ and $\phi(t)$ to visualize the modification to $\phi_A(t)$ caused by the cross-coupling. (This comparison was shown in figure 3 of [6].)

Since the Sjögren model can explain the nearly logarithmic decay dynamics observed in the OKE data close to T_C, it seems worthwhile to explore its ability to explain other aspects of structural relaxation dynamics in molecular glass-forming liquids as well. This possibility was already considered in 1988 by Götze, Sjögren, and co-workers (although not in the context of rotation–translation coupling) who identified a new feature in the spectrum corresponding to $\phi_A(t)$ not predicted by the basic MCT, a high-frequency β peak located between the susceptibility minimum and the microscopic (boson) peak [52]. They also showed that this feature, in leading-order asymptotic expansion, corresponds to the Cole–Cole function.

4.2. The Sjögren model and the excess wing

While analysing the OKE data for BZP [6], Sperl noted that the corresponding $\chi''_A(\omega)$ spectrum exhibited an excess wing [53]. Starting from his parameters, we have generated a series of theoretical susceptibility spectra $\chi''_A(\omega)$ first by reducing the separation parameter $\varepsilon = (T - T_C)/T_C$ (equivalent to lowering T) while keeping all other parameters fixed, and second by increasing the RT coupling constant V_A while keeping all other parameters fixed. (In fitting real data, all three parameters would be expected to change with changing temperature.)

In figure 4 we show orientational susceptibility spectra $\chi''_A(\omega)$ computed with the Sjögren model using four values of the separation parameter $\epsilon = -0.8$, -0.4, -0.2, and -0.1. (The Sjögren model parameters used to generate the spectra in figures 4 and 5 are shown in table 1.) For all four spectra there is a region above the α peak with a reduced slope. Power law fits to the spectra in this excess wing region are shown together with CD fits to the α peaks, and the slope decreases as ε (and therefore $T - T_c$) decreases, a result that is consistent with the results of Leheny and Nagel [18]. Note that for $\varepsilon = -0.1$, which corresponds to the lowest temperature, the excess wing is beginning to exhibit an incipient β peak.

In figure 5, we show the effect of increasing the RT coupling constant V_A while holding all other parameters fixed. For the smallest V_A ($V_A = 10$), the excess wing is flat and shows no sign of a secondary peak. As V_A increases to 30, 60, and 100, a distinct secondary peak

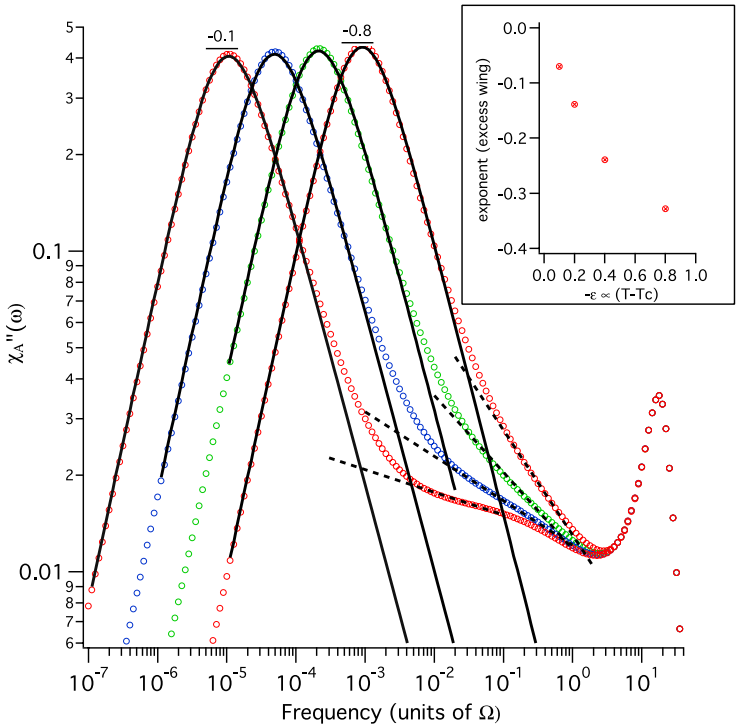

Figure 4. The orientational susceptibility function $\chi''_{\rm A}(\omega)$ from the Sjögren model (equations (4.3)) for separation parameters (right to left) $\varepsilon = -0.8$, -0.4, -0.2, and -0.1 (circles) with $V_{\rm A}$ fixed at 30. ($\varepsilon = (T_{\rm C} - T)/T_{\rm C}$ denotes the dimensionless separation of T from the MCT crossover temperature $T_{\rm C}$.) Parameters used in figures 4 and 5 are listed in table 1. CD fits to the α peaks extrapolated to high frequencies are shown as solid curves. Power law fits to the excess wing are shown as dashed lines. The exponents found in the fits are shown in the inset. Note that with decreasing $(T - T_{\rm C})$ the excess wing slope decreases as observed in the dielectric experiments discussed in the text.

Table 1. Parameters used to construct figures 4 and 5 from equations (4.3) ($\gamma = \gamma_{\rm A} = 17.5$; $\lambda = 0.70$; $V_1^C = 0.816$; $V_2^C = 2.041$).

Figure 4	$\Omega = \Omega_{\rm A}$	V_1	V_2	$V_{\rm A}$
$\varepsilon = -0.1$	3.5	0.793	1.996	30
$\varepsilon = -0.2$	3.5	0.773	1.946	30
$\varepsilon = -0.4$	3.5	0.741	1.833	30
$\varepsilon = -0.8$	3.5	0.689	1.573	30
Figure 5	$\Omega = \Omega_{\rm A}$	V_1	V_2	$V_{\rm A}$
$\varepsilon = -0.1$	1.0	0.793	1.996	10
$\varepsilon = -0.1$	1.0	0.793	1.996	30
$\varepsilon = -0.1$	1.0	0.793	1.996	60
$\varepsilon = -0.1$	1.0	0.793	1.996	100

develops in the same region. Thus, the evolution of the excess wing into a JG β peak reported by Lunkenheimer *et al* [30] and by Reiser *et al* [35] is reproduced here, and indicates that this transformation can be a consequence of the increase of the RT coupling strength which would be expected to occur with increasing pressure which causes the density to increase.

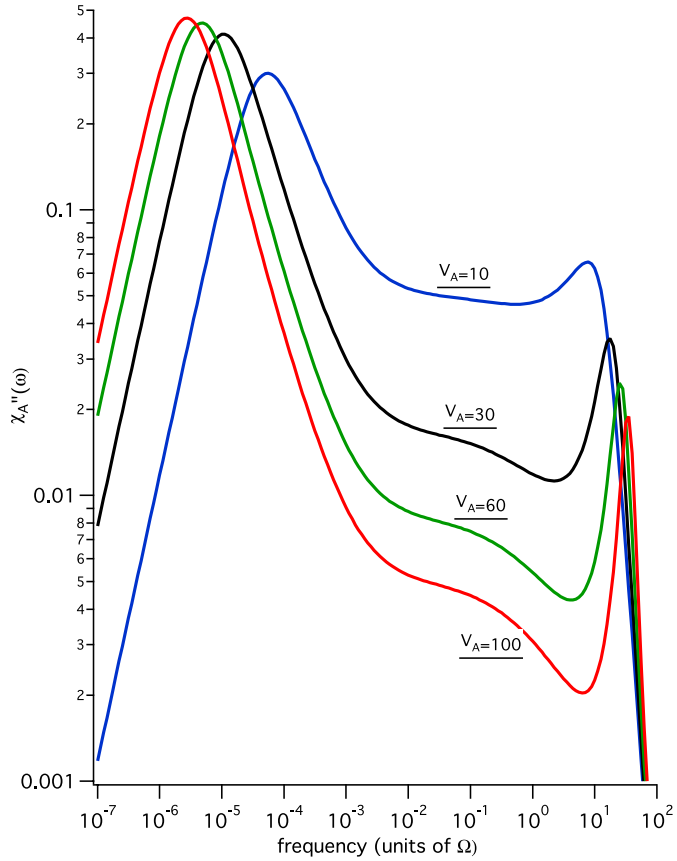

Figure 5. The effect on the susceptibility spectrum of increasing the rotation–translation coupling constant V_A with all other parameters held constant. The excess wing at $V_A = 10$ gradually transforms with increasing V_A to a weak JG β peak at $V_A = 100$ as discussed in the text.

4.3. Sjögren model fits to PC dielectric spectra

Finally, we attempted to use the Sjögren model to fit the experimental PC dielectric spectra shown in figure 1. We note that the excess wing, and especially the β peak, only begins to appear at temperatures below the MCT crossover temperature $T_C \sim 187$ K. The Sjögren model can be solved for $T < T_C$ using the extended MCT (EMCT) which includes activated hopping, as reported for PC by Götze and Voigtmann [54]. However, currently available versions of the extended theory approximate the activated hopping function $\Delta(\omega)$ by a frequency-independent hopping constant Δ. Solutions to these equations for $T < T_C$ can describe the region of the minimum correctly but do not exhibit realistic α peaks or excess wings [55]. These fits were therefore not successful.

5. Conclusions

In this communication we have suggested that the secondary structure frequently observed in the high-frequency wing of the α peak in dielectric or light scattering spectra of glass-forming liquids may be a consequence of rotation–translation coupling. We have shown

that susceptibility spectra calculated with the two-correlator schematic MCT Sjögren model exhibit features qualitatively resembling those seen in experimental spectra. In particular, the decrease in the slope of the excess wing with decreasing temperature and the transformation of the excess wing into a β peak, both of which have been observed in experiments, are shown to be a natural consequence of the model. Unfortunately, we have not been able to produce satisfactory fits to actual experimental data because the secondary structure is primarily observed at temperatures below T_C where the model is not sufficiently accurate for simultaneously describing the microscopic dynamics and the structure of the α relaxation region.

Acknowledgments

We thank P Lunkenheimer for providing the dielectric data shown in the figures. We thank W Götze, M Sperl, T Voigtmann and M Fuchs for many helpful discussions and for providing computer programs for solving the MCT Sjögren model equations. We thank E Rössler, A Brodin, K Ngai, N Menon, R Torre, M Goldstein, M Roland, and R Pick for helpful suggestions and correspondence, and Y F Song for help with computer programming. This material is based on work supported by the National Science Foundation under grant number DMR-0243471.

References

[1] Brodin A, Bergman R, Mattsson J and Rössler E A 2003 *Eur. Phys. J.* B **36** 349
[2] Rösner P, Sawmer K and Lunkenheimer P 2004 *Europhys. Lett.* **68** 226
[3] Stegeman G I A and Stoicheff B P 1968 *Phys. Rev. Lett.* **21** 202
Stegeman G I A and Stoicheff B P 1973 *Phys. Rev.* A **7** 1160
Enright G D and Stoicheff B P 1976 *J. Chem. Phys.* **64** 3658
[4] Zhang H P, Brodin A, Barshilia H C, Shen G Q, Cummins H Z and Pick R M 2004 *Phys. Rev.* E **70** 011502
[5] Dreyfus C, Aouadi A, Pick R M, Berger T, Patkowski A and Steffen W 1998 *Europhys. Lett.* **42** 55
Dreyfus C, Aouadi A, Pick R M, Berger T, Patkowski A and Steffen W 1999 *J. Phys.: Condens. Matter* **11** A139
Dreyfus C, Aouadi A, Pick R M, Berger T, Patkowski A and Steffen W 1999 *Eur. Phys. J.* B **9** 401
Dreyfus C, Aouadi A, Gapinski J, Matos-Lopez M, Steffen W, Patkowski A and Pick R M 2003 *Phys. Rev.* E **68** 011204
Pick R M, Franosch T, Latz A and Dreyfus C 2003 *Eur. Phys. J.* B **31** 217
Franosch T, Latz A and Pick R M 2003 *Eur. Phys. J.* B **31** 229
[6] Götze W and Sperl M 2004 *Phys. Rev. Lett.* **92** 105701
Sperl M 2005 unpublished
[7] Cang Hu, Novikov V N and Fayer M D 2003 *Phys. Rev. Lett.* **90** 197401
Cang Hu, Novikov V N and Fayer M D 2003 *J. Chem. Phys.* **118** 2800
[8] Compare Lunkenheimer P, Schneider U, Brand R and Loidl A 2000 *Contemp. Phys.* **41** 15
[9] Davidson D W and Cole R H 1951 *J. Chem. Phys.* **19** 1484
[10] Goldstein M 2004 private communication
[11] Goldstein M 1969 *J. Chem. Phys.* **51** 3728
[12] Johari G P and Goldstein M 1970 *J. Phys. Chem.* **74** 2034
[13] Johari G P and Goldstein M 1970 *J. Chem. Phys.* **53** 2372
[14] Johari G P and Goldstein M 1971 *J. Chem. Phys.* **55** 4245
[15] Wong J and Angell C A 1974 *Glass: Structure by Spectroscopy* (New York: Dekker) pp 722–3
[16] Lunkenheimer P and Loidl A 2003 *Phys. Rev. Lett.* **91** 207601
[17] Sokolov A P, Kisliuk A, Novikov V N and Ngai K 2001 *Phys. Rev.* B **63** 172204
[18] Leheny R L and Nagel S R 1998 *J. Non-Cryst. Solids* **235–237** 278
[19] Adichtev S, Blochowicz T, Gainaru C, Novikov V N, Rössler E A and Tschirwitz C 2003 *J. Phys.: Condens. Matter* **15** S385
[20] Blochowitz Th, Tschirwitz Ch, Benkhof St and Rössler E A 2003 *J. Chem. Phys.* **118** 7544

[21] Adichtev S, Blochowicz T, Tschirwitz C, Novikov V N and Rössler E A 2003 *Phys. Rev.* E **68** 011504
[22] Lunkenheimer P, Pimenov A, Scheiner B, Böhmer R and Loidl A 1996 *Europhys. Lett.* **33** 611
[23] Lunkenheimer P, Pimenov A, Dressel M, Goncharov Yu G, Böhmer R and Loidl A 1996 *Phys. Rev. Lett.* **77** 318
[24] Lunkenheimer P, Pimenov A, Dressel M, Gorshunov B, Schneider U, Schiener B, Böhmer R and Loidl A 1997 *Mater. Res. Symp. Proc.* **455** 47
[25] Schneider U, Brand R, Lunkenheimer P and Loidl A 2000 *Eur. Phys. J.* E **2** 67
[26] Ngai K L, Lunkenheimer P, Leon C, Schneider U, Brand R and Loidl A 2001 *J. Chem. Phys.* **115** 1405
[27] Schneider U, Lunkenheimer P, Brand R and Loidl A 1999 *Phys. Rev.* E **59** 6924
[28] Lunkenheimer P, Wehn R, Riegger Th and Loidl A 2002 *J. Non-Cryst. Solids* **307–310** 336
[29] Brand R, Lunkenheimer P, Schneider U and Loidl A 2000 *Phys. Rev.* B **62** 8878
[30] Schneider U, Brand R, Lunkenheimer P and Loidl A 2000 *Phys. Rev. Lett.* **84** 5560
[31] Blochowicz T and Rössler E A 2004 *Phys. Rev. Lett.* **92** 225701
[32] Oh J-Y and Hwang Y-H 2005 in preparation
[33] Ngai K L and Paluch M 2004 *J. Chem. Phys.* **120** 857
[34] Casalini R and Roland M 2003 *Phys. Rev. Lett.* **91** 015702
Casalini R and Roland M 2004 *AIP Conf. Proc.* **708** 523
[35] Reiser A, Kasper G and Hunklinger S 2004 *Phys. Rev. Lett.* **92** 125701
[36] Lunkenheimer P, Schneider U, Brand R and Loidl A 1999 *Slow Dynamics in Complex Systems: Eighth Tohwa University International Symposium* (*AIP Conf. Proc.* No. 469) ed M Tokuyama and I Oppenheim (New York: AIP) p 433
[37] Wiedersich J, Surovtsev N V and Rössler E 2000 *J. Chem. Phys.* **113** 1143
[38] Kudlik A, Benkhof S, Lenk R and Rössler E 1995 *Europhys. Lett.* **32** 511
[39] Bengtzelius U, Götze W and Sjölander A 1984 *J. Phys. C: Solid State Phys.* **17** 5915
[40] Götze W 1991 *Liquids, Freezing, and the Glass Transition* (*Les Houches Lectures*) (Amsterdam: North-Holland) p 289
[41] Götze W and Sjögren L 1992 *Rep. Prog. Phys.* **55** 241
[42] Götze W 1999 *J. Phys.: Condens. Matter* **11** A1
[43] Götze W 1984 *Z. Phys.* **56** 139
[44] Compare Chong S H and Götze W 2002 *Phys. Rev.* E **65** 041503
Chong S H and Götze W 2002 *Phys. Rev.* E **65** 051201
Schilling R 2002 *Phys. Rev.* E **65** 051206
Theenhaus T, Schilling R, Latz A and Letz M 2001 *Phys. Rev.* E **64** 051505
Latz A, Letz M, Schilling R and Theenhaus Th 2002 *J. Non-Cryst. Solids* **307–310** 172
[45] Fuchs M, Götze W and Mayr M R 1998 *Phys. Rev.* E **58** 3384
[46] van Megen W, Mortensen T C, Williams S R and Müller J 1998 *Phys. Rev.* E **58** 6073
[47] Sperl M 2005 submitted
[48] Sjögren L 1986 *Phys. Rev.* A **33** 1254
[49] Hinze G, Brace D D, Gottke S D and Fayer M D 2000 *Phys. Rev. Lett.* **84** 2437
[50] Wiebel S and Wuttke J 2002 *New J. Phys.* **4** 56.1
[51] Ricci M, Wiebel S, Bartolini P, Taschin A and Torre R 2004 *Phil. Mag.* **84** 1491
[52] Buchalla G, Dersch U, Götze W and Sjögren L 1988 *J. Phys. C: Solid State Phys.* **21** 4239
Götze W and Sjögren L 1989 *J. Phys.: Condens. Matter* **1** 4183
[53] Sperl M 2004 private communication
[54] Götze W and Voigtmann Th 2000 *Phys. Rev.* E **61** 4133
[55] Voigtmann T 2004 private communication